International Journal of Nanoelectronics and Materials
Volume 12, No. 3, July 2019 [291-308]

Promoting the Aggregation and Disaggregation Dynamic of Superparamagnetic Nano-Particles

N. Maleki-jirsaraei[1*], S. Kabi[1] and S. Azizi[1]

[1]*Physics Department, Alzahra University, P.O. Box 1993891176, Tehran, Iran.*

Received 25 August 2018, Revised 17 January 2019, Accepted 26 February 2019

ABSTRACT

In this study the behavior of nano magnetite colloid particles with polystyrene coated in the presence of an external magnetic field was investigated. It is observed that the average cluster size and the number of clusters show a power law behavior with time, both in aggregation and disaggregation processes. Adding sodium dodecyl sulfate (SDS) change during coated process the value of z and z', the dynamical exponents' of power law, and has optimum value. At this value the aggregation and disaggregation exponents are almost equal, z~ź.

Keywords: Aggregation, Disaggregation, Super-paramagnetic, Polystyrene, Sodium Dodecyl Sulfate

1. INTRODUCTION

Magneto Rheological (MR) fluids have attracted the attention of many authors in the last two decades. MR fluids are a suspension of magnetic colloidal nano particle which are dispersed in a carrier fluid. These colloidal particles are made of Iron or Cobalt which have magnetic properties, there is a Van der Waals force between the particles and results in an irreversible link and the suspension is unstable. The surfactant is used to have a stable suspension; The choice of surfactant depends on the type of carrier fluid and its application [1] [2]. Due to their unique properties, such as thermal, rheological, magnetic and electrical properties, they are widely used in industry and medicine [3] [4] [5]. This is due to their special properties in the presence of magnetic fields. The fluids also change from solid phase to liquid in the presence of external magnetic field [6]. The most important property of these fluids is its response to the magnetic field, even within a short time (about milliseconds), which is the basis of many scientific and practical advances in this field. The magnetic field causes the particles to be polarized and, as a result, causes particles to oscillate. In the absence of the magnetic field, the particles have a relatively low cluster size. In some cases, carrier fluid can be a suspension of nanoparticles or, in other words, Ferro fluid. An interesting phenomenon happens when the system is super-paramagnetic. This happens when each particle is only a magnetic field, and if the particle size is less than 20 nm, we will observe this event [7]. In the super-paramagnetic phase, when the external magnetic field H illuminates, the nano-particles begin to collapse into the chain structures, because their dipole magnetic period, are matched. The magnetic dipole period M, of a typical nano-particle, is VM, where M=xH is the magnetization of the particle, x is particle's magnetic susceptibility and V is the volume of the particles [8] [9] [10]. When the external magnetic field is switched off, the particles start to move due to Brownian forces which makes the chains disappear, hence the nano-particles disaggregate quickly [11] leading to zero magnetization. These processes are especially important for practical usage such as designing

*Corresponding Author: *maleki@alzahra.ac.ir*

on-off devices based on magnetic fluids [12] [13]. Because of particle super-paramagnetic, this system has turned into a functional substance. [14] [15]. Because of their magnetic dipole moments and electric surface forces, magnetic nano-particles will aggregate without coating [16] [17] [18]. However, coating them with non-magnetic materials such as poly-styrene and SDS can prevent unwanted (strict or columbic) forces between particles. The role of the van der Waals force in magnetite nanoparticles is more important than the magnetic interactions of particles.

The role of the van der Waals force in magnetite nanoparticles is more important than the magnetic interactions of particles. The surfactant (layer stabilizer) prevents this paraphrasing and clogging through a short-range repulsion between particles (strep repulsion) in an intermediate solvent. If the intermediate solvent is of the hydrocarbon type, per sulphide stability is achieved through surfactant or polymer. In dilute magnetic fluids, when used as an intermediate solvent, the electrostatic cracking induced by surfactant and non-magnetic material such as the polymer can cause fossil floating and the dispersion of nanoparticles in water. In practice, OH bonds appear on the poly-styrene coating and cause polarization of some of the particles. After turning off the magnetic field, Brownian and electrostatic forces cause particles to separate [19] [20]. Research continues to find particles that have better magnetic properties, super-parametric, so that the system can respond faster to the magnetic field.

1.1 Theory

A suspension of well coated magnetic nano-particles behaves like a super-paramagnet. Under the influence of an external magnetic field, the particles rapidly align and produce a sizable magnetization. After turning off the magnetic field they quickly rearrange themselves to random orientations.

Neglecting the gravitational forces (the particles are floating in a suspensions), the total force exerted by the jth particle on the ith particle $\vec{F}_{ij}$ has three components, the magnetic force $\vec{F}_{ij}^{m}$ that drives the aggregation process and excluded-volume force $\vec{F}_{ij}^{EV}$that prevents a particle to overlap with another particle, and a Brownian term $\vec{F}_{ij}^{B}$ due to thermal fluctuations. For the magnetic force, the point-dipole approximation is [21]:

$$\vec{F}_{ij}^{m} = \frac{3\mu_0 m^2}{4\pi}\sum_{i\neq j}\frac{1}{r_{ij}^4}\left\{\left[1-5(\hat{m}.\hat{r}_{ij})^2\right]\hat{r}+2(\hat{m}.\hat{r}_{ij})\hat{m}\right\} \quad (1)$$

Where $\vec{r}_{ij} = \hat{R}_i - \hat{R}_j, \hat{r}_{ij} = \vec{r}_{ij}/r_{ij}$ is the unitary vector between the center of mass of particles *i* and *j*. The excluded-volume and the Brownian terms respectively are:

$$\vec{F}_{ij}^{EV} = A\frac{3\mu_0 m^2}{4\pi(2a)^4}\sum_{i\neq j} exp\left[-B\left(\frac{r_{ij}}{2a}-1\right)\right]\hat{r}_{ij} \quad (2)$$

and

$$\langle F_{il}^{B}(t)F_{i'j'}^{B}(t')\rangle = 2D\delta(t-t')\delta_{ii'}\delta_{jj'} \quad (3)$$

Where D is the diffusion coefficient and the subscript l corresponds to the spatial directions, l=x, y, z [8] [21].

Bulk particles and nano-particles show different behaviour in an external magnetic field. Bulk particles react to an external field by movement of their domain walls, while uniaxial nano-

particles show spins rotation. The energy barrier, ΔE, exists in system with anisotropies. Since those particles' spin shows a preference for certain directions, their energy landscapes contain minima in the preferred directions and maxima in the least preferred directions.

The preferred axis of a particle with uniaxial anisotropy is commonly referred to as easy axis and there are two minima: one for each direction along the easy axis.

According to the Néel–Brown model, the mean time spent in one state of magnetization is given by an Arrhenius law [22]:

$$\tau = \tau_0 \, exp\left(\frac{\Delta E}{k_b T}\right) \tag{4}$$

Where τ_0 is the fluctuation time, which is about $\tau_0 \sim 10^{-9}$ seconds and τ is the relaxation time- time needed to go from one minimum to the other- which can be in the range $\approx \tau_0$ - ∞, since τ increases exponentially with decreasing temperature. In other words it is unlikely that an escape process will be observed at low temperatures. But when the energy barrier is sufficiently small, i.e. comparable with thermal energy, which is in the case of super-paramagnetic particles, the particle's magnetization can fluctuate between the two orientations [15, 17].

$$N\,(t) = \sum_s n_s\,(t) \tag{5}$$

and S (t) represents the average cluster size at time t

$$S\,(t) = \frac{\sum_s n_s\,(t)\, s^2}{\sum_s n_s\,(t)\, s} \tag{6}$$

Both parameters $N\,(t) \sim t^{-z'}$ and $S\,(t) \sim t^{z}$ follow power law behaviour;

Also we can describe the standard deviation of cluster size at time t, with parameter l(t):

$$l\,(t) = \frac{\sum_s n_s(t) s^2}{N(t)} \quad , \qquad l\,(t) \sim t^{z'} \tag{7}$$

According to the dynamic scaling theory we have [23]:

$$n_s\,(t) \sim t^{-w} s^{-\tau} f\left(\frac{s}{t^{\tau}}\right) \tag{8}$$

Alternatively:

$$n_s\,(t) \sim s^{-2} g\left(\frac{s}{t^{z}}\right) \tag{9}$$

Here *f(x)* is a scaling function with $f(x) \cong 1$ for $x \ll 1$ and $f(x) \ll 1$ for $x \gg 1$ and *g(x)* is a scaling function with $g(x) \ll 1$ for $x \gg 1$ and $g(x) \sim x^{\Delta}$ for $x \ll 1$, where Δ is named the crossover exponent.

The number of particles that do not participate in aggregation is given by $n_I(t)$, the following relation holds, as we can see they have power law behaviour with the time

$$n_I\,(t) \sim t^{-w} \tag{10}$$

The relation between w, z and Δ is given by:

$$\Delta = \frac{w}{z} \tag{11}$$

So Δ can be obtained by two methods, by plotting *g(x) vs. x=S/t z,* and by obtaining *w* and *z* and using Eq. (10), we checked these two methods and found them compatible [24].

2. MATERIAL AND METHODS

2.1 Sample Preparation

Magnetite nanoparticles are synthesized by chemical coprecipitation method from $FeCl_2$-$4H_2O$ and $FeCl_3$-$6H_2O$. Oleic acid has been used as surfactant and polystyrene as nanoparticle coatings. More information can be found in Maleki et al study [25]. Then nanoparticles with polystyrene were covered with methylene chloride and sodium dodecyl sulphate (SDS) in vacuum. The salt SDS can also act as surfactant; so there are dual surfactants. The particles are functionalized with carboxylic groups. The shapes of these particles are almost ideally spherical with very smooth surfaces

2.2 Experimental Setup

The schematic diagram a shows our experiment set up to record the accumulation and degradation of Magneto Rheological (MR) fluids, as well as suspension of nanoparticles coated with polystyrene and water under an external magnetic field of 1.2 *mT*. The suspension achieved between two quartz windows was limited to 2μm. We also used a digital CCD camera (Kc-7H1P) and a video microscopy (B-353, magnification 140000, rating 85V to 256V, 50/60 Hz).

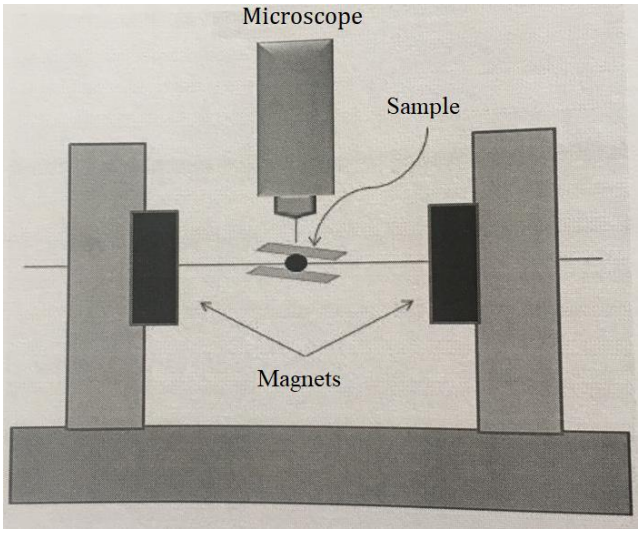

Diagram A: the schematic of experiment set up for observation of aggregation and disaggregation of MR fluids under an external magnetic field

3. RESULTS AND DISCUSSION

3.1 Magnetite Nanoparticles with Polystyrene

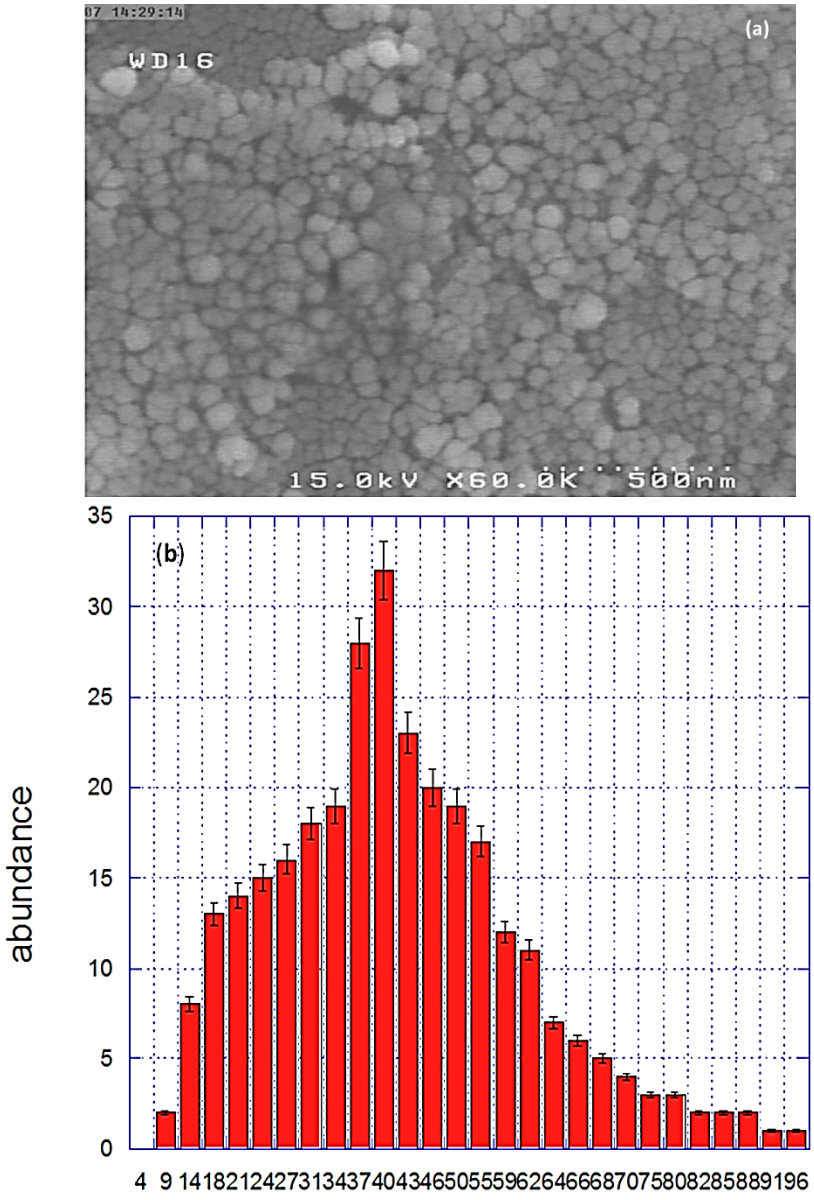

Figure 1. (a) SEM image of Fe3O4 nano-particles coated by Ps and Oleic acid as surfactant with Magnify of 100000 times in air without any vacuum. (b) Size distribution of these particles which shows the average size is about 36nm.

Figure 1(a) shows the SEM result of the nanoparticles for the distribution of the sample size as mentioned in Section 2.1.The particle size distribution shown in Figure 1(b) is derived from the SEM image of Figure 1(a) and plotted using the Kgraph software. The average particle size also is about 36 nm.

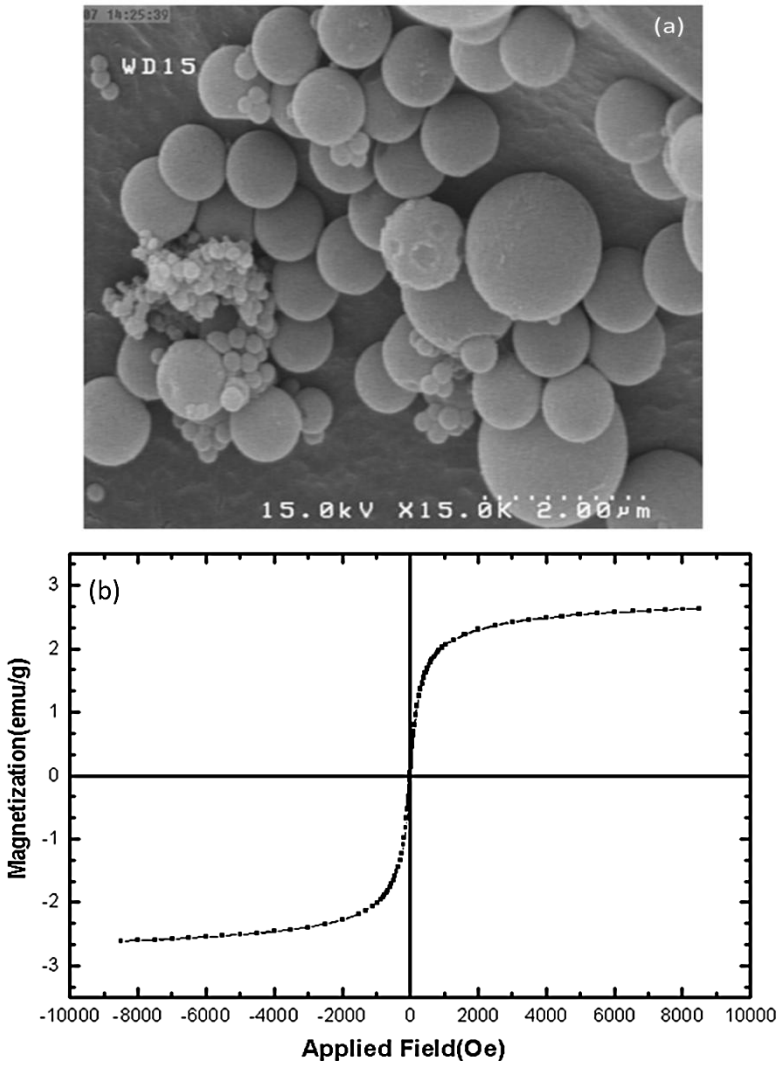

Figure 2. (A) SEM images of nano-particles coated with poly-styrene in vacuum , in the scale of 2 µm and 15000 magnification and (B) Magnetization vs. applied field curve from VSM technique for the magnetic particles with the magnetic saturation 2.8 (emu/g).

Figure 2(a) shows the SEM images of the micrometre-sized coated super-paramagnetic particles (Fe3O4 coated with polystyrene (PS)). We observed that the shape of these particles is almost spherical with very smooth surfaces. The magnetic properties of these particles have been shown in Figure 2(b) with a magnetic saturation of 2.8 (emu/g). We used the FTIR spectroscopy to recognize coated nano-particles with poly-styrene (Fe3O4/PS).

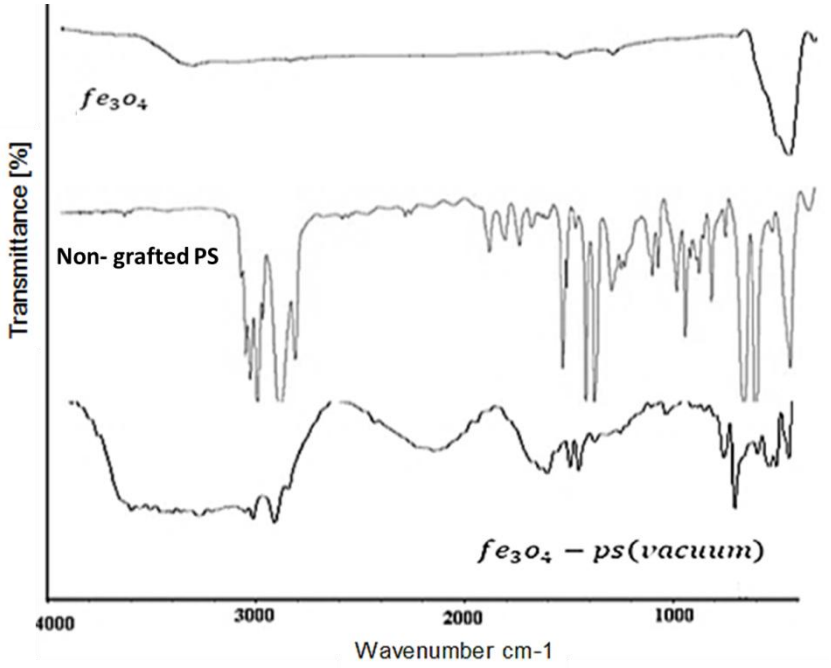

Figure 3. Difference between the FTIR spectroscopy for magnetite nanoparticle, normal poly-styrene and nano-particles coated with poly-styrene in vacuum for up to down respectively.

Figure 3 shows the difference between the FTIR spectroscopy for magnetite, normal poly-styrene and nano-particles coated with poly-styrene in vacuum. There is a peak in 750cm^{-1} for –NH groups and in 1000 cm^{-1} for C=O groups and in 1480cm^{-1} related to CH3 groups, which confirm the existence of poly-styrene coated layer on magnetite.

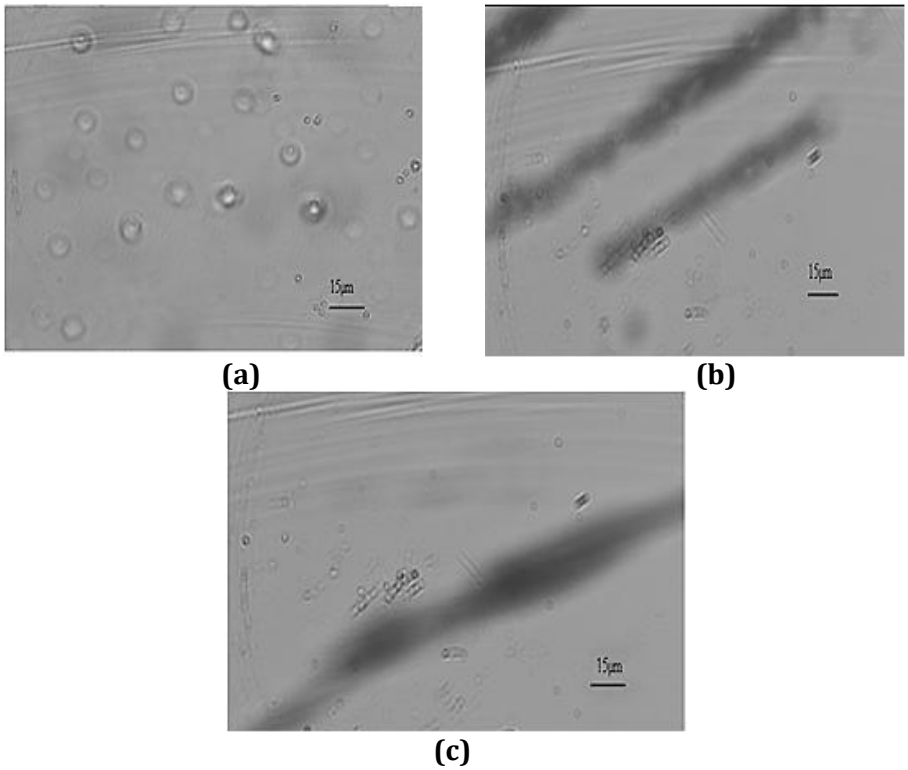

Figure 4. The graph of aggregation of coated nano-particles, at different times (a) t=0s, (b) t=600s and (c) t=1680s after a magnetic field B=1.2 mT was turned on.

As shown in Figure 4, in the presence of external field the particles align themselves along the direction of the external field and aggregation is brought about. Over time more particles participate in the aggregation process and we can see the regime of cluster-cluster aggregation, which lowers the number of clusters. Since the process is happening in a thin layer, the system of particles is two-dimensional (2D) and consequently, we focus the imaging system on the layer of particles located right above the bottom quartz window.

3.2 Aggregation

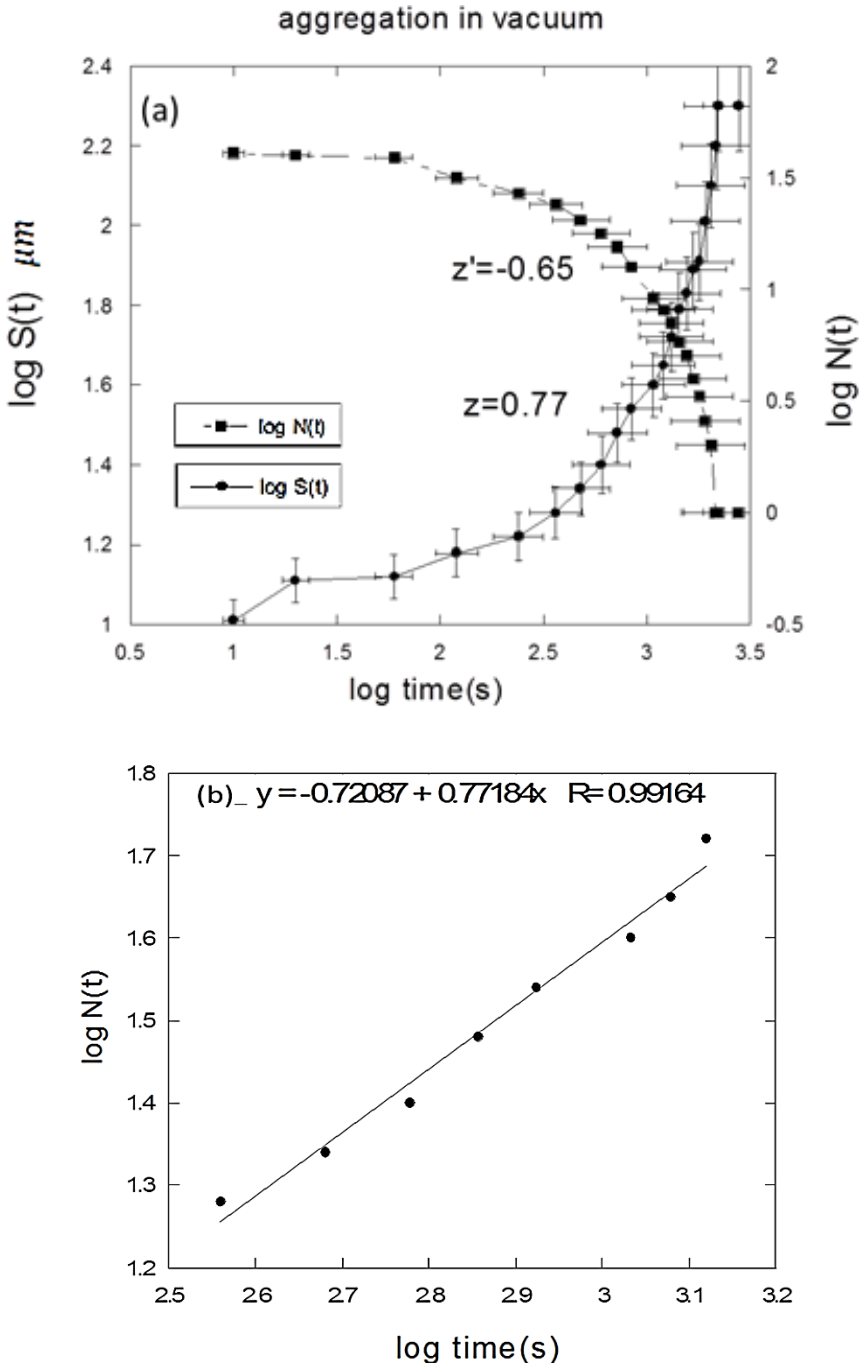

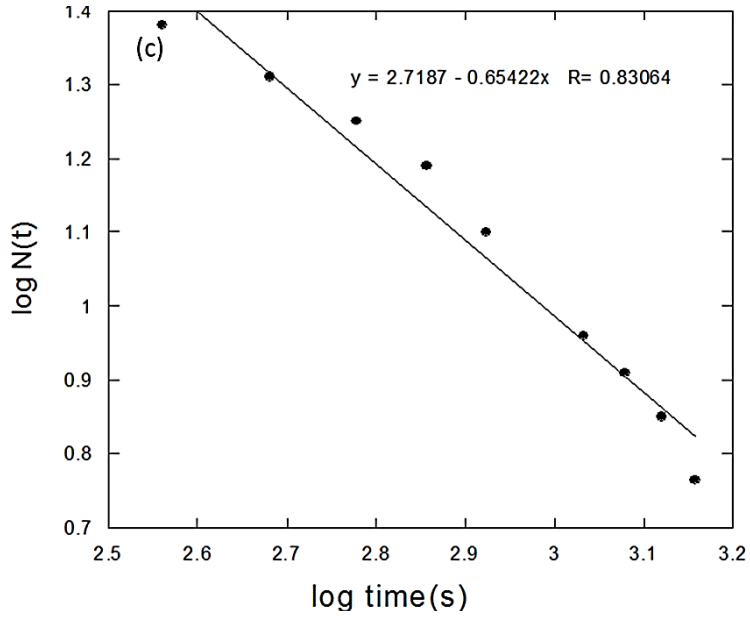

Figure 5. (a) N(t),the number of clusters, and S(t), the average clusters size, as a function of time. both obeys a power law behavior with time, (b) The power law behavior between S(t) over time which specifically represent the manner of z, (c) The power law behavior of N(t) over time which specifically represent the manner of z'.

In this section the size of the clusters $S(t)$ was measured, which was formed under the influence of the magnetic field and as well as cluster size distribution was calculated at the time, $N(t)$; That was done by taking films of processes via the camera of a microscope. In Figure 5 was shown the plot log $S(t)$ and log $N(t)$-the size and number of the clusters- as a function of time. And also shows the power law behavior of them after a while, in the regime of cluster-cluster aggregation.

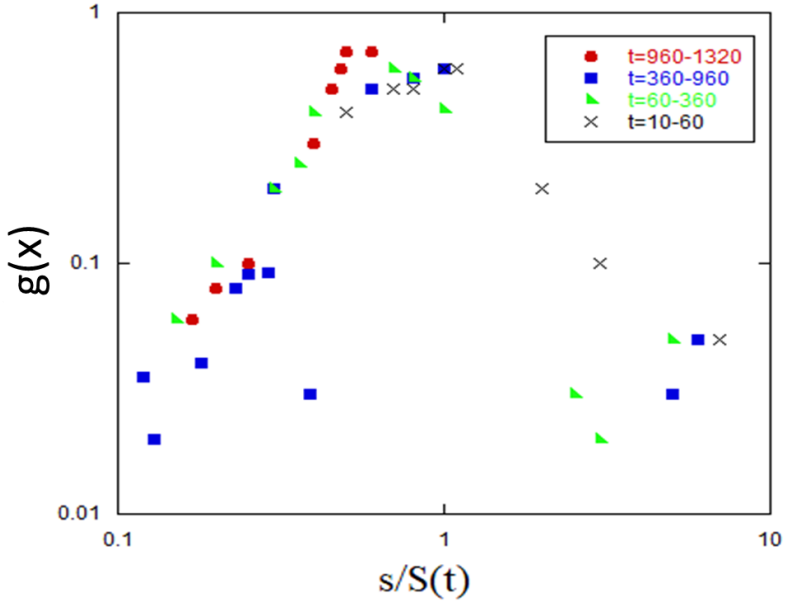

Figure 6. $g(x) = s^2 n_s(t)$ vs. $s/S\,(t)$, for x<1 and t> 60s the data have been fitted to a power law g(x) ~x^{Δ} with exponent Δ=1.8±0.1.

Furthermore the value of the two parameters z and z' equal to z=0.77±0.10 and z'=0.65±0.01. Therefore, based on the value of the defined parameters, figure 6 shown the plot of the function $g(x) = s^2 n_s(t)$ from the measured data in experiments, against $s/S(t)$ that gives us the cross over exponent Δ (see eq.11) , meaning that for each samples at the specific time in this case t>60s, the data have been fitted to a power law behavior $g(x) \sim x^{\Delta}$, see figure 6 , on the other hand for time t>60s where the average cluster size, $S(t)$ obeys a power law, the data scale properly with a cross over Δ=1.8±0.1 for $s/S(t)$ <1.

3.3 Dis-Aggregation

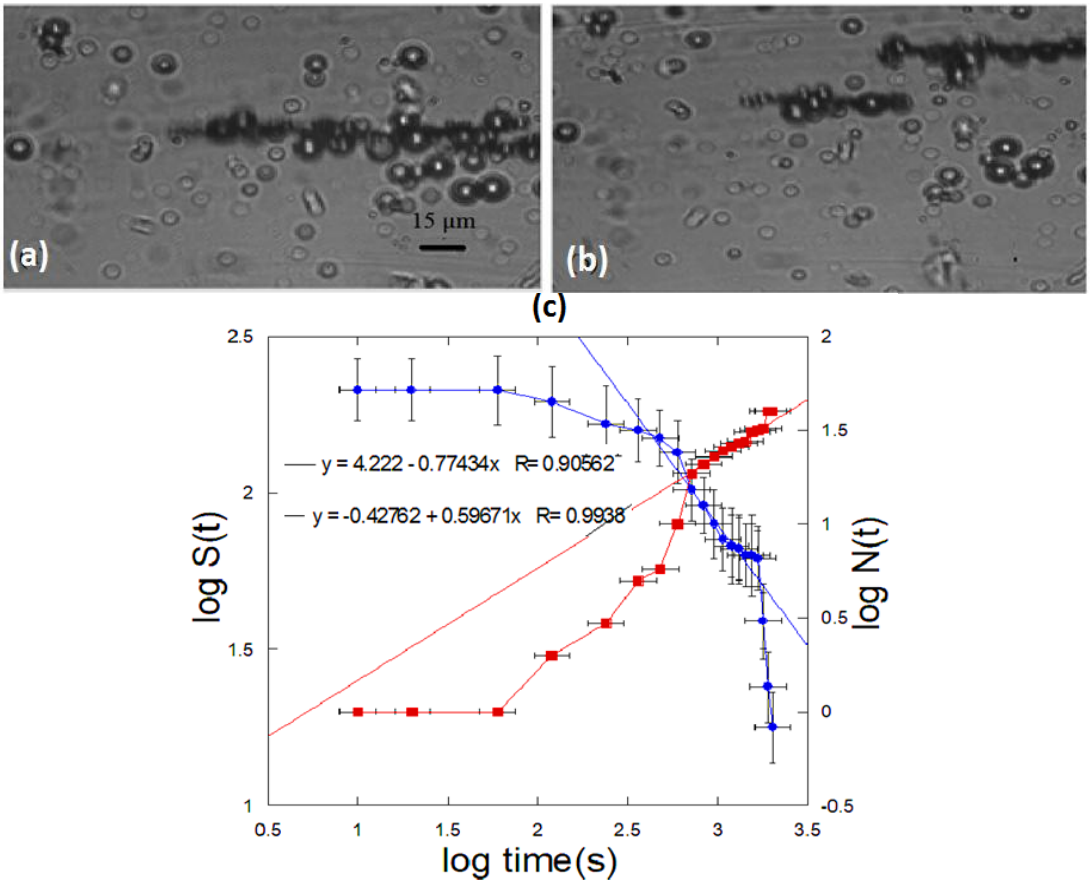

Figure 7. The reverse process in dispersing the chains (a) 10s, (b) 600s after the magnetic field was disconnected and (c) Represent disaggregation process and the values of $S(t)$ and $N(t)$.

When the external magnetic field is turned off, the particles start to leave the chains due to Brownian forces and over time the chains disappear. Figure 7 presents the disaggregation in the time range of (10s-600s) after the magnetic field was turned off. As well as shows the whole process of disaggregation in the reverse of the aggregation process $S(t) \sim t^{-z}$,$N(t) \sim t^{z'}$, and figure 7.c shows the value of z=0.77±0.01 and z'=0.60±0.01.

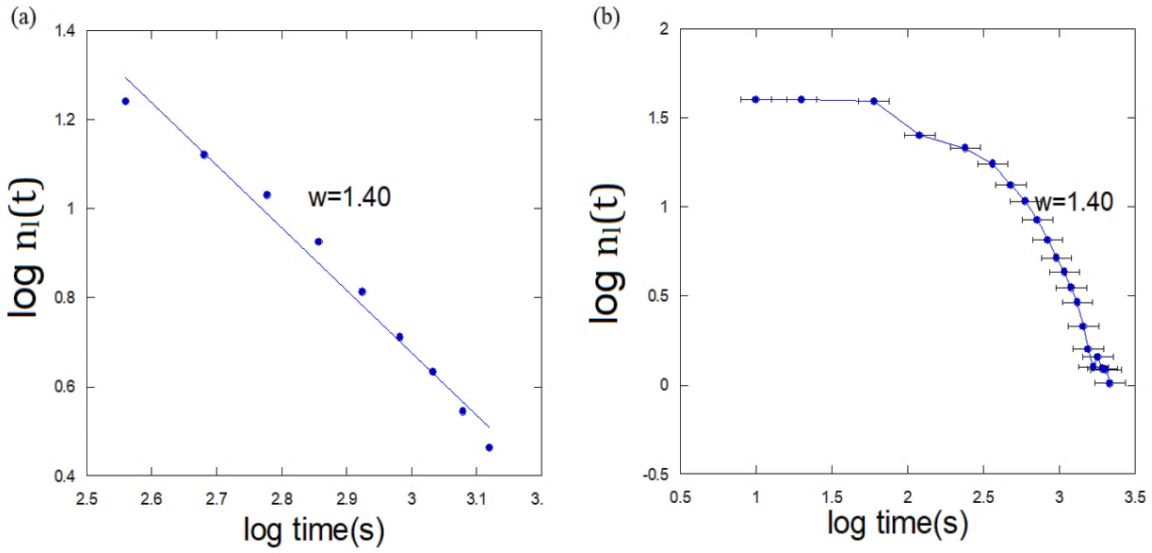

Figure 8. The power law behavior of $n_l(t)$ with time and, w=1.40±0.02.

Figure 8 also shows the power law behavior of the number of particles that do not participate in aggregation, in agreement with Eq. (10). In this figure we can obtain the parameter *w*, which is important because of its relationship with *z* and *Δ*, according to the Eq. (11).

Table 1 The three kind experiments with 30mg of SDS and specially the relationship between the important exponents of w, Δ and z according to Equation (11)

z	z´	w	Δ	Δ=w/z
0.65±0.01	0.82±0.01	1.18±0.01	1.8±0.2	1.81
0.77±0.10	0.65±0.01	1.14±0.03	1.5±0.1	1.48
0.94±0.04	0.85±0.10	1.40±0.02	1.3±0.1	1.4

According to Table 1 with the value of 30 mg SDS, the amount of the parameter Δ obtained by the first method which is based on relation$g(x)\sim x^{\Delta}$ (Figure 6) is about the same as the second method which is based on Eq. (10) and Eq. (11) (Figure 8) and parameters *z* and *w*, according to the equation $w = z\Delta$.

Having the state of $z \approx \dot{z}$ is suitable target and this component is closer to unity, it's best to application as an on-off switches which has the same low relaxation time for both on-off cases. Adding KCl to the suspension resulted in a better mode for switching off (disaggregation) but the aggregation state led to more delay time, so adding KCl was not helping towards the ideal switch.

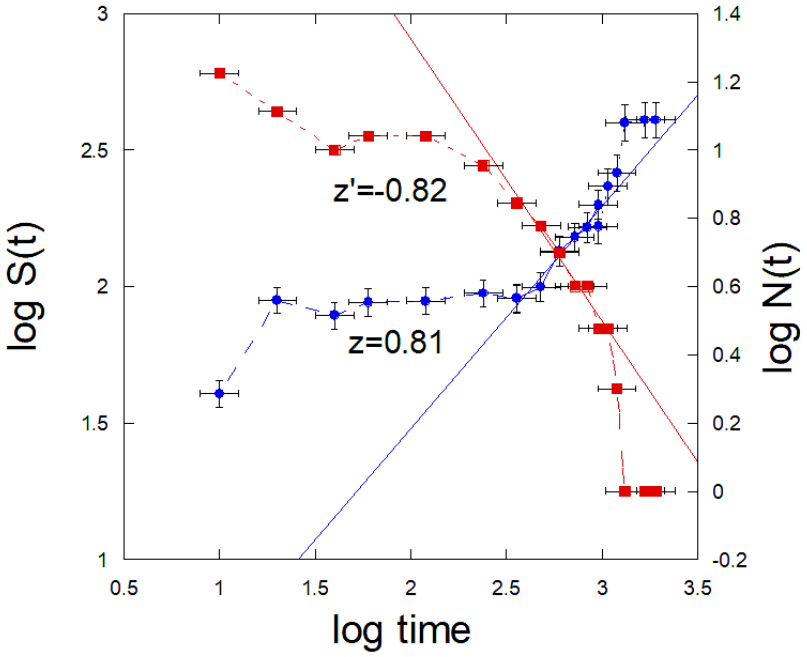

Figure 9. The power law behavior with 20mg of sodium dodecyl sulfate (SDS), in this case, s, $z \approx z'$ which is close to ideal.

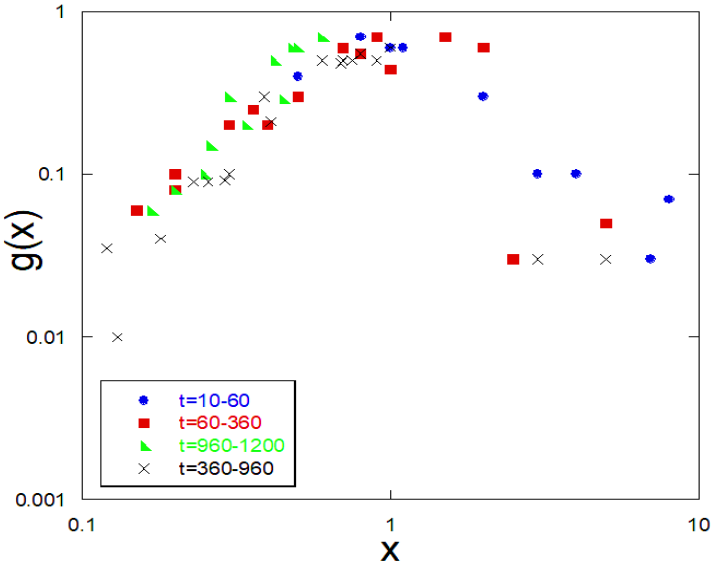

Figure 10. The scaling function $g(x) = s^2 n_x$ (t) obtained from cluster size distributions n_s (t) with 20mgSDS, the data have been fitted to a power law $g(x) \sim x\Delta$ with exponent Δ=1.98 ±0.04.

As shown in figure 9, the results on aggregation with 20mg of SDS presents the values $< z >= 0.81 \pm 0.0$ and $< z' >= 0.82 \pm 0.08$, which are significantly higher kinetic exponent values than the other amounts of SDS that we used to prepare the sample. The results for the sample prepared with 20 mg SDS are shown in Figure 9 and 10, and results for all 5 samples are summarized in Tables 2 and 3 below.

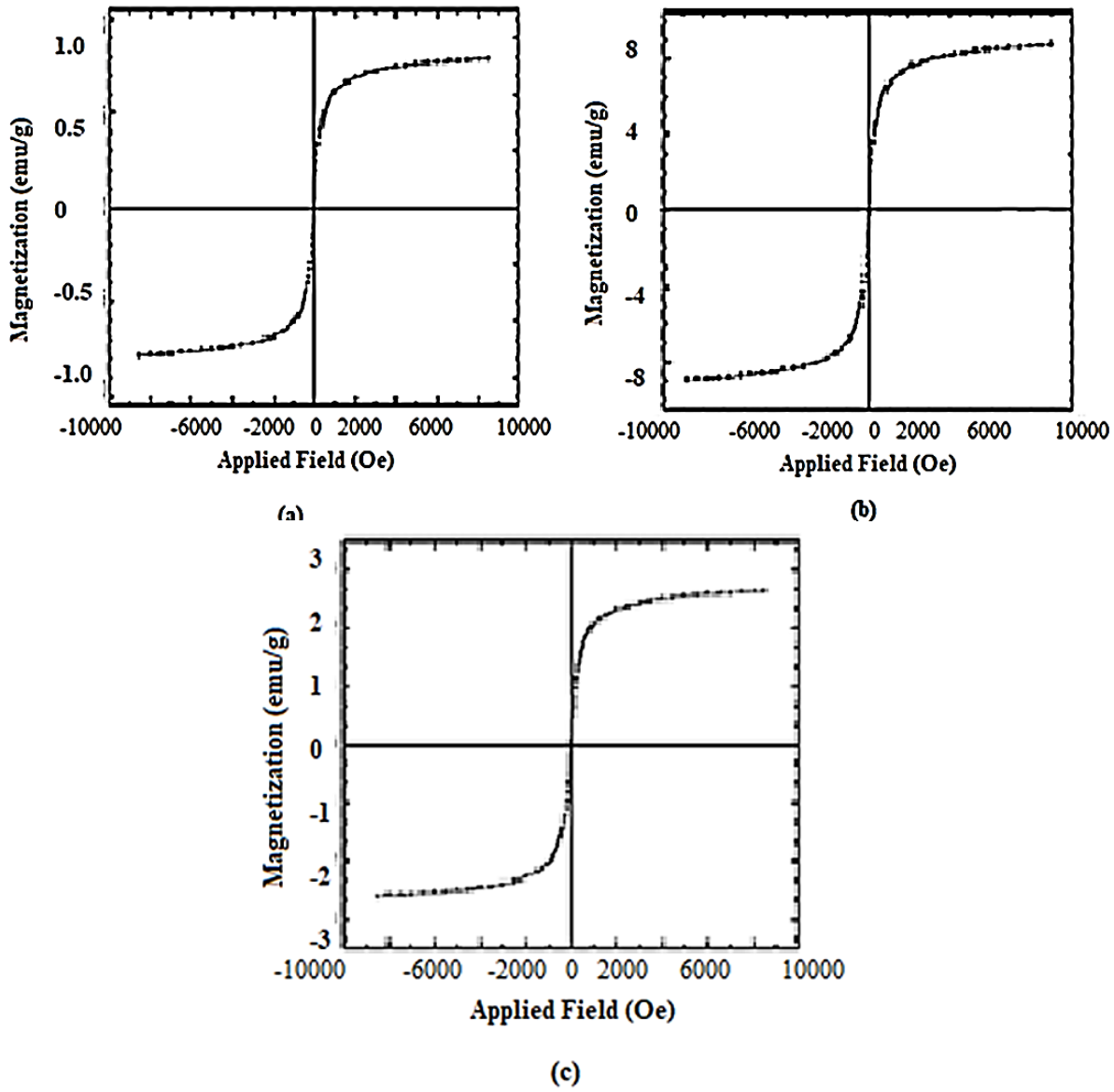

Figure 11. VSM plots for 3 samples prepared with 3 levels of SDS, (A) 10mg, (B) 20mg and (C) 30mg. as can be seen from the figures, the magnetic saturation level is the highest for 20mg SDS.

When the amount of SDS is high, it coats almost all of the nano-particles and it makes the poly-styrene coat the particles individually which results in a good super-paramagnetic behavior but a low dipole moment, see figure 11.a.

When the amount of SDS is not enough for helping the poly-styrene coat all the individual particles in one core, it makes the poly-styrene coat a few of the particles together in a single core, so the dipole moment is the average of the particles coated in one core and it's not high due to their random directions, so the super-paramagnetic behavior is not pronounced, due to the high mass and small magnetization, figure 11.b.

But when SDS has an optimal amount between these two states, number of the particles forming one core is more than one but not much higher, this causes their dipole moment to be almost in the same direction which results in a relatively high magnetization whereas the core is still small so low mass, and therefore has a good super-paramagnetic behavior. Figure 11(C)

This optimal amount for SDS at 20mg was found. The sample sensitized with this amount of SDS had the best results and the closeness of Z, Z' to each other and unity was the highest recorded. And all of its dynamical exponents are the nearest to the ideal amounts among all reported results.

Table 2 The summary of the whole experiment in aggregation mode with five levels of substance SDS (10, 15, 20, 25, and 30 mg). The ideal situation $(z \approx z')$ in the level of 20mg SDS

Aggregation		
Amount of SDS(mg)	Z	Z´
10	0.36±0.10	0.46±0.01
	0.43±0.01	0.57±0.03
	0.55±0.05	0.69±0.07
15	0.51±0.04	0.65±0.01
	0.58±0.01	0.65±0.01
20	0.81±0.01	0.82±0.01
	0.93±0.3	0.94±0.2
	0.95±0.01	0.97±0.03
25	0.79±0.02	0.84±0.01
	0.80±0.01	0.85±0.01
		0.82±0.01
30	0.65±0.01	
	0.77±0.10	0.65±0.01
	0.94±0.04	0.85±0.10

Table 3 The summary of the whole experiment in Disaggregation mode with five levels of substance SDS (10, 15, 20, 25, and 30 mg). The ideal situation $(z \approx z')$ in the level of 20mg SDS

Disaggregation		
amount of SDS(mg)	Z	Z´
10	0.57±0.01	0.60±0.02
	0.62±0.02	0.72±0.01
	0.63±0.1	0.72±0.01
15	0.63±0.02	0.68±0.04
	0.69±0.01	0.73±0.03
20	0.85±0.01	0.87±0.4
	0.89±0.02	0.90±0.01
	0.93±0.03	0.95±0.01
25	0.79±0.02	0.84±0.01
	0.78±0.05	0.84±0.03
30	0.82±0.01	0.89±0.04
	0.62±0.03	0.73±0.01
	0.65±0.01	0.73±0.01

Table 4 The summarized amount of Δ obtained by plotting g(x) versusx^{Δ}

Amount of SDS(mg)	Δ
10	1.4±0.1 1.1±0.2 0.8±0.4
15	1.5±0.3 1.3±0.1
20	1.98±0.04 2.01±0.1 2±0.1
25	1.7±0.2 1.6±0.1
30	1.8±0.2 1.5±0.1 1.3±0.3

As seen in Tables 3 and 4 and figure 11, for the samples prepared with 20mg SDS the optimum mode occurs. The cross over exponent can be obtained using scaling function $g(x)$ plotted against s/S(t). The resulting values for Δ are summarized in Table 4, as can be seen we have $z \approx \acute{z}$ then Δ≅ 2 , this means that we should have the best value of Δ in the time range in which S(t) shows power law behavior and $z \approx z'$, this happens for 20mg of substance SDS.

4. CONCLUSION

In this paper the aggregation and disaggregation of nano-magnetite colloids coated with poly-styrene suspended in fluids, in the presence of an external magnetic field was observed. Also, we presented that the number of clusters and the average length of clusters have power law behaviors with time, both in aggregation and disaggregation, and was obtained the dynamical exponents.

In this study it was found that the SDS reduces the surface charge of the nano-particles and helps coating them with poly-styrene, it was also found experimentally that the ratio of SDS and polystyrene and the concentration of nano-particles is important.

We synthesized Iron oxide nano-particles by co-precipitation method and added oleic acid as the surfactant. To avoid particle aggregation before applying magnetic field, we coated poly-styrene on nano-particles in vacuum condition, which resulted in much higher quality magnetic beads. The structure, size and magnetic properties of the samples were defined by means of VSM, SEM and FTIR spectroscopy. We found that the amount of SDS in the process of sample preparation is important and it has an optimum amount, of 20 mg. The sample made with this amount of SDS resulted in the best dynamical exponent, i.e. aggregation and disaggregation exponents equalize, $z \sim \acute{z}$ and are near to unity, and Δ is approximately 2, thus we achieved the best results so far, which means the lowest response time in both aggregation and disaggregation. This outcome enables one to design much better magnetic on-off switches.

ACKNOWLEDGEMENT

We would like to thank Professor Daniel Bonn and Professor Shahin Rouhani for their collaboration. This work has been supported by the Center of International Scientific Studies & Collaboration (CISSC). We appreciate member of the Complex Systems Laboratory of Al-Zahra University for their cooperation.

REFERENCES

[1] CV Biju, MS Shunmugam, "Development of a boring bar with magneto rheological fluid damping and assessment of its dynamic characteristics," Journal of Vibration and Control, (2017) 3094-3106.

[2] Y Liang, J R. Alvarado, Kl D. Iagnemma & A.E. Hosoi, "Dynamic Sealing Using Magnetorheological Fluids," Physical Review Applied, (2018) 064049.

[3] Le-Duc, Thang, Vinh Ho-Huu & Hung Nguyen-Quoc, "Multi-objective optimal design of magnetorheological brakes for motorcycling application considering thermal effect in working process," Smart Materials and Structures, (2018) 27.

[4] SW Cha, SR Kang, YH Hwang, JS Oh, "A controllable tactile device for human-like tissue realization using smart magneto-rheological fluids: fabrication and modeling," Smart Materials and Structures , Smart Materials and Structures **27.6** (2018).

[5] Ahamed, Raju, Seung-Bok Choi & Md Meftahul Ferdaus., "A state of art on magneto-rheological materials and their potential applications," Journal of Intelligent Material Systems and Structures **29** (2018) 2051-2095.

[6] P. Domínguez-GarcíaJ. M. PastorM. A. Rubio, "Aggregation and disaggregation dynamics of sedimented and charged superparamagnetic micro-particles in water suspension," The European Physical Journal E **4** (2011) 36.

[7] Knopp, T. Buzug, T. M, Magnetic particle imaging: an introduction to imaging principles and scanner instrumentation, Verlag Berlin Heidelberg: Springer, (2012).

[8] P. Domínguez-García, Sonia Melle, J. M. Pastor & M. A. Rubio, "Scaling in the aggregation dynamics of a magnetorheological fluid," Physical Review E **76** (2007) 051403.

[9] P Smirnov, F Gazeau, M Lewin, JC Bacri, "In vivo cellular imaging of magnetically labeled hybridomas in the spleen with a 1.5-T clinical MRI system," Magnetic Resonance in Medicine: An Official Journal of the International Society for Magnetic Resonance in Medicine **52.1** (2004) 73-79.

[10] R. A. Kerr, Science **247** (1990) 050401.

[11] CJ Chin, S Yiacoumi, C Tsouris, "Agglomeration of magnetic particles and breakup of magnetic chains in surfactant solutions," Colloids and Surfaces A: Physicochemical and Engineering Aspects **274** (2002) 63-72.

[12] JC Fernández-Toledano, M Tirado-Miranda, J Baudry, "Kinetic study of coupled field-induced aggregation and sedimentation processes arising in magnetic fluids," Physical Review E **78.1** (2008) 011403.

[13] Larson, R. G. Arbor, A, Oxford University Press, (1999).

[14] Khuat N. T., Nguyen V. A. T., Phan T. -N., Thach C. V., Hai N. H., Chau N., "Extension of the Inhibitory Effect of Chloramphenicol on Bacteria by Incorporating It into Fe∼ 3O∼ 4 Magnetic Nanoparticles," Journal-Korean Physical Society **52** (2008) 1323.

[15] J Černák, G Helgesen, AT Skjeltor, "Aggregation dynamics of nonmagnetic particles in a ferrofluid," Physical Review E **70** (2004) 031504.

[16] E. SasitoSarwodidoyo, "Study Of CuZnFerrite and Ferrofluid In The Flow Injection Synthesis," Advances in Social Sciences Research Journal **4** (2007).

[17] S. Charles, "The preparation of magnetic fluids," Ferrofluids, (2002) 3-18.

[18] MC Miguel, R Pastor-Satorras, "Kinetic growth of field-oriented chains in dipolar colloidal solutions," Physical Review E **59** (1999) 826.

[19] F. Martínez-Pedrero, M. Tirado-Miranda, A. Schmitt & J. Callejas-Fernández, "Formation of magnetic filaments: A kinetic study," Physical Review E **76** (2007) 011405.

[20] T. Vicsek & F. Family, "Dynamic scaling for aggregation of clusters," Physical Review Letters **52** (1984).

[21] W. Brown, "Thermal fluctuations of a single-domain particle," Physical Review **1677** (1963) 130.

[22] L. Néel, Selectec Works of Louis Néel, Gordon and Breach Science Publishers, (1988).

[23] P Meakin, T Vicsek, F Family, "Dynamic cluster-size distribution in cluster-cluster aggregation: Effects of cluster diffusivity," Physical Review B **31** (1985) 564.

[24] J Panyam, V Labhasetwar, "Biodegradable nanoparticles for drug and gene delivery to cells and tissue," Advanced drug delivery reviews **55** (2003) 329-347.

[25] Maleki-Jirsaraei, N. Ghane-Motlagh, B. Ghane-golmohamadi, F. Ghane-Motlagh, R. Rouhani, "Synthesis and analysis of the properties of ferro-fluids," in Nanoscience and Nanotechnology International Conference, (2010).